ChemComm

COMMUNICATION

View Article Online
View Journal | View Issue

Cite this: *Chem. Commun.*, 2025, **61**, 5443

Received 28th January 2025,
Accepted 4th March 2025

DOI: 10.1039/d5cc00528k

rsc.li/chemcomm

Towards water-tolerant *ansa*-aminoboranes for parahydrogen-induced polarization and beyond†

Karolina Konsewicz,[a] Timo Repo [b] and Vladimir V. Zhivonitko *[a]

Three orders of magnitude of ^{1}H NMR signal enhancement were observed in the metal-free activation of parahydrogen using an *ansa*-aminoborane in the presence of a 100-fold water excess at 9.4 T. Kinetic studies corroborated the reversibility of water addition to the intramolecular N–B Lewis centers in both polar and nonpolar solvents. Furthermore, DFT modeling supported these results.

Allowing for metal-free activation of small molecules,[1] *ansa*-aminoboranes (AABs), as an example of intramolecular frustrated Lewis pairs (FLPs),[2–5] show remarkable reactivity towards dihydrogen.[6–11] This feature can open new horizons in catalysis based on more sustainable main group elements,[3] which has already been demonstrated through AAB-catalyzed hydrogenation reactions of various substrates such as imines and alkynes under mild conditions.[8,9] In addition to the catalytic applications, it has been documented that AABs show prominent nuclear spin hyperpolarization in activations of parahydrogen (para-H_2),[12–15] the spin-0 nuclear spin isomer of H_2, utilized for dramatic NMR sensitivity enhancement through the so-called parahydrogen-induced polarization (PHIP).[16–18] Typically, precious metal complexes are employed to generate PHIP,[19,20] whereas AABs can provide metal-free alternatives. Furthermore, the amine–borane functionality carried by these species can be adopted as a platform for the molecular design of organic functional groups that generate PHIP. However, AABs are very sensitive to traces of moisture and typically quench through the formation of inactive Lewis adducts with water.[21,22]

In general, the moisture sensitivity problem of FLPs has attracted attention since the transition from research to industrial settings requires certain stability levels of the catalysts.[23] For instance, it has been demonstrated that variation of substituent bulkiness in the aromatic rings of tri(aryl)boranes can lead to suitable water tolerance of the Lewis acidic boron center to perform catalytic hydrogenations and reductive aminations of carbonyl compounds in water-containing solvents.[24,25] AABs have not been reported yet to have any remarkable water tolerance. To the contrary, these species were considered water intolerant,[21] which stimulated a search for other FLP systems with *ansa* scaffolds that could have more favorable properties.[21,22] These activities led to the invention of an *ansa*-phosphinoborane with cyclohexyls at the phosphine site that demonstrated activation of dihydrogen in the presence of 6 equivalents of H_2O.[21] However, it was found that at the same time water reduction occurs as a side reaction leading to the formation of the corresponding phosphine oxide. The latter problem could be resolved if one could find a water-tolerant AAB, since the nitrogen center is not prone to oxidation.

Herein, we report that a previously known orthophenylene-bridged AAB with two mesityl substituents at the boryl site (1-(2-(dimesitylboraneyl)phenyl)-2,2,6,6-tetramethylpiperidine, **MesCAT**)[12] demonstrates strong nuclear spin hyperpolarization effects upon activation of para-H_2 in acetonitrile in the presence of more than two orders of magnitude excess of water (Fig. 1A). The observation of PHIP proved undoubtedly that **MesCAT** demonstrates water tolerance. The observed signal enhancements for the generated **MesCAT-H_2** adduct exceeded three orders of magnitude at 9.4 T. Interestingly, changing mesityls to phenyl substituents leads to completely irreversible quenching of the AAB active center (Fig. 1B), highlighting the importance of balance between steric effects and Lewis acidity. We envision that further rational design can lead to efficient water-tolerant AABs for para-H_2 activation.

Initial hyperpolarization experiments were performed using a 1 mM solution of ^{15}N-labelled **MesCAT** adduct with water, **MesCAT-H_2O**, in water-containing acetonitrile-d3 with H_2O concentration of 0.1 M, see ESI† for details. The **MesCAT-H_2O**÷H_2O ratio was 1÷100, so there was a significant excess of water present in the unbound form in solution. The presence

[a] *NMR Research Unit, Faculty of Science, University of Oulu, P.O. Box 3000, Oulu, 90014, Finland. E-mail: vladimir.zhivonitko@oulu.fi*
[b] *Department of Chemistry, University of Helsinki, A. I. Virtasen aukio 1, Helsinki, 00014, Finland*

† Electronic supplementary information (ESI) available: Experimental materials and methods; para-H_2 experiments and 1D EXSY NMR data; supporting ^{1}H and ^{11}B NMR spectra; theory and DFT results; *xyz* structures. See DOI: https://doi.org/10.1039/d5cc00528k

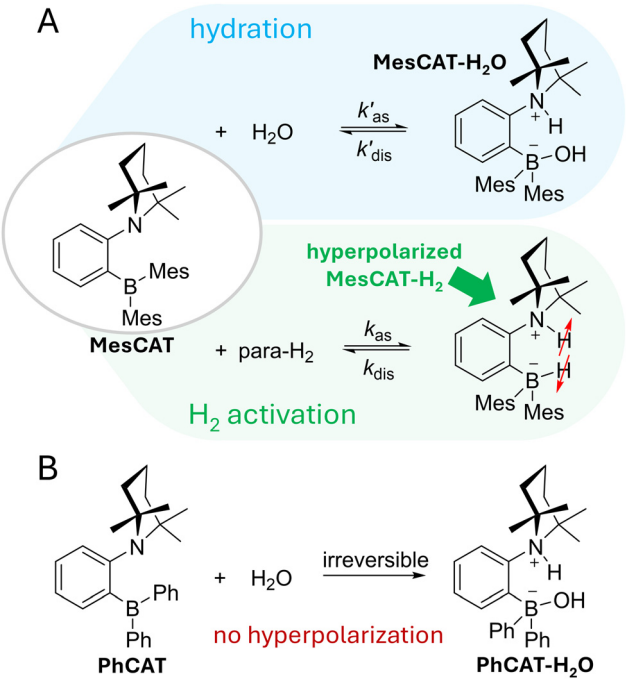

Fig. 1 (A) Dynamic hydration (pink background) and H_2 activation (green background) equilibria that lead to the interconversion between free **MesCAT**, its water adduct **MesCAT-H_2O**, and hyperpolarized **MesCAT-H_2** in the reaction mixture initially containing **MesCAT-H_2O**, water in excess, and para-H_2. (B) Irreversible hydration of **PhCAT** that completely quenches the reactivity of this AAB through the formation of the inactive **PhCAT-H_2O** water adduct, thereby disabling hyperpolarization.

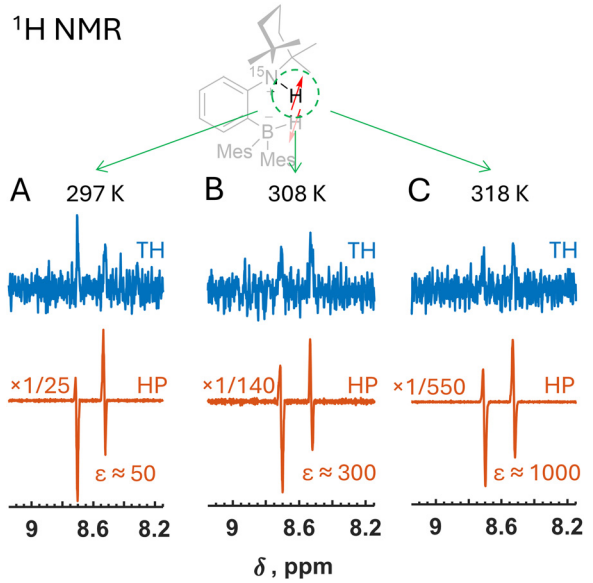

Fig. 2 Thermal (TH, red) and hyperpolarized (HP, blue) ^{1}H NMR spectra measured in the experiments with a 2.3 mM solution of ^{15}N-labelled **MesCAT-H_2O** charged with 6 bars of para-H_2 in acetonitrile-d3 at (A) 297, (B) 308, and (C) 318 K. The NH group resonances corresponding to **MesCAT-H_2** are depicted in the figure. These species were generated in the solution due to the dynamic equilibria shown in Fig. 1A. Enhancement factors, ε, and multiplication factors used for signal amplitude scaling are indicated for the hyperpolarized spectra. The spectra were acquired using $\pi/4$-pulses to maximize the amplitudes of the hyperpolarized signals (PASADENA condition).[18] The thermal spectra were measured after the complete relaxation of the samples to thermal equilibrium.

of free H_2O was evident from ^{1}H NMR spectra shown in the ESI† (Fig. S1). The follow-up experiments with para-H_2 were performed by charging 6 bars of para-H_2 (*ca.* 92%) to this solution in a gas-tight NMR tube, shaking, and transferring the sample into the magnet for the acquisition of spectra; see ESI† for details. Already at room temperature, this procedure resulted in the observation of hyperpolarization effects in the ^{1}H NMR spectra (Fig. 2A). The room temperature signal enhancement for the NH group proton in the **MesCAT-H_2** adduct was about 50. However, heating the sample to 308 K led to more pronounced signal enhancement of more than two orders of magnitude (*ca.* 300-fold), as shown in Fig. 2B. Heating to 318 K produced even higher enhancements (*ca.* 1000-fold, Fig. 2C). Further heating to 328 K resulted in the further increase of the enhancement factor to *ca.* 1500 (see Table 1). For all temperatures, ^{11}B NMR revealed an enhanced antiphase signal corresponding to the hyperpolarized boron site in **MesCAT-H_2** (Fig. S4 in ESI†), a feature[13,14] commonly present in the activation of para-H_2 with various orthophenylene AABs. We also note that increasing the **MesCAT-H_2O**$\div H_2O$ ratio is expected to raise the equilibrium concentration of **MesCAT-H_2**, boosting the absolute amplitudes of both its thermal and hyperpolarized ^{1}H signals. A general discussion of this effect can be found in the ESI† (Section S1.7). However, a detailed study is beyond the scope of this communication and will be addressed in future work.

Table 1 Estimated ^{1}H NMR signal enhancement factors for the **MesCAT-H_2** NH group and selected kinetic parameters obtained from 1D EXSY NMR for the equilibria in Fig. 1

Solvent	T, K	ε, enh. factor	k'_{dis}, s^{-1}	k_{dis},[a] s^{-1}
Acetonitrile	297	50 ± 10	2.3 ± 0.2	0.032 ± 0.002
	308	300 ± 50	8.0 ± 0.6	0.12 ± 0.02
	318	1000 ± 200	23 ± 2	0.38 ± 0.04
	328	1500 ± 300	64 ± 5	1.1 ± 0.2
Toluene	297	>400	14 ± 1	2.4 ± 0.3
	308	>600	63 ± 5	7.8 ± 0.9

[a] Data taken from ref. 15.

Interestingly, similar experiments with **PhCAT-H_2O**, the phenyl analogue of **MesCAT-H_2O**, and para-H_2 in acetonitrile-d3 showed no hyperpolarization effects in ^{1}H NMR spectra in the temperature range from 297–328 K (Fig. S23–S27 in ESI†). At the same time, it was demonstrated previously that **PhCAT-H_2** provides similar ^{1}H NMR signal enhancements to **MesCAT-H_2**.[15] The enhanced boron resonances for hyperpolarized **PhCAT-H_2** were also not visible in ^{11}B NMR. Generally, measured ^{1}H and ^{11}B NMR spectra did not reveal any changes after the addition of para-H_2 to the reaction solution, implying that the dissociation of **PhCAT-H_2O** and adduct and the subsequent formation of the hyperpolarized **PhCAT-H_2** did not take place.

To discuss these results, it is convenient to consider the sequence of events leading to the hyperpolarized **MesCAT-H_2** in Fig. 1A. Being inactive towards H_2 activation as such, **MesCAT-H_2O** must dissociate to release a sensible amount of **MesCAT** species that in turn can activate para-H_2. Therefore, an important prerequisite for the hyperpolarization is the presence of the two dynamic equilibria in the solution: (1) **MesCAT-H_2O** dissociation and (2) facile para-H_2 activation by **MesCAT**. **MesCAT** is the key intermediate in this process, while the ability of **MesCAT-H_2O** to dissociate is a critical feature that enables the formation of this intermediate. Considering this process from the general perspective, one must have reversible hydration (upper equilibrium for **MesCAT** in Fig. 1A) of AAB to observe hyperpolarization effects, a feature that is absent in the case of **PhCAT-H_2O** (Fig. 1B).

In this context, it is essential to know the kinetic parameters of the equilibria and details of the hyperpolarization mechanism. The reaction rate measurements performed using the 1D EXSY NMR technique provided data about the exchange process between bound water in **MesCAT-H_2O** and free water in the solution (Table 1; see ESI† for experimental details). The exchange rates are seen to increase with increasing the temperature, as expected. Generally, we can conclude also that the lifetimes of the **MesCAT-H_2O** species in the presence of the equilibrium shown in Fig. 1A are on the order of tens to hundreds of milliseconds. Such rather short lifetimes make the exchange between **MesCAT** and **MesCAT-H_2O** reversible enough to observe polarization effects for **MesCAT-H_2**, which is formed in another reversible process of para-H_2 activation, Fig. 1B. A detailed discussion of para-H_2 activation for **MesCAT** and other AABs in acetonitrile was reported recently in ref. 15 and will not be considered here any further. However, the comparison of the dissociation rate constants for **MesCAT-H_2O** (k'_{dis}) and **MesCAT-H_2** (k_{dis}) in Table 1 reveals that the lifetimes, defined as the inverse of the rate parameters, of the former species are at least an order of magnitude shorter as compared to those of the latter species. In other words, one can conclude that **MesCAT-H_2O** is less stable than **MesCAT-H_2**. Apparently, this feature of **MesCAT** facilitates the observation of nuclear spin hyperpolarization effects with para-H_2 for **MesCAT-H_2**.

In addition to acetonitrile-d3, **MesCAT-H_2O** and **PhCAT-H_2O** were examined in toluene-d8 in terms of PHIP effects. In this case, the excess of water was significantly lower (AAB-$H_2O \div H_2O$ ratio was *ca.* $1 \div 7$) due to the limited solubility of H_2O in toluene. Similarly to acetonitrile experiments, strong hyperpolarization of the generated **MesCAT-H_2** species was observed in the case of **MesCAT-H_2O** in toluene with signal enhancements exceeding two orders of magnitude at 9.4 T (Table 1; see Fig. S5 and details in ESI†). The kinetic measurements revealed even more facile reversibility of water addition in toluene than in acetonitrile since the corresponding water dissociation constant, k'_{dis}, was 6–8 times lower at the same temperatures in the former case. It is clear that the reversibility of water addition is an intrinsic feature of **MesCAT**. In contrast, the experiment with **PhCAT-H_2O** in toluene did not result in any hyperpolarization, and there was no sign of reversibility of water addition to **PhCAT** for the temperatures up to 328 K examined in this study.

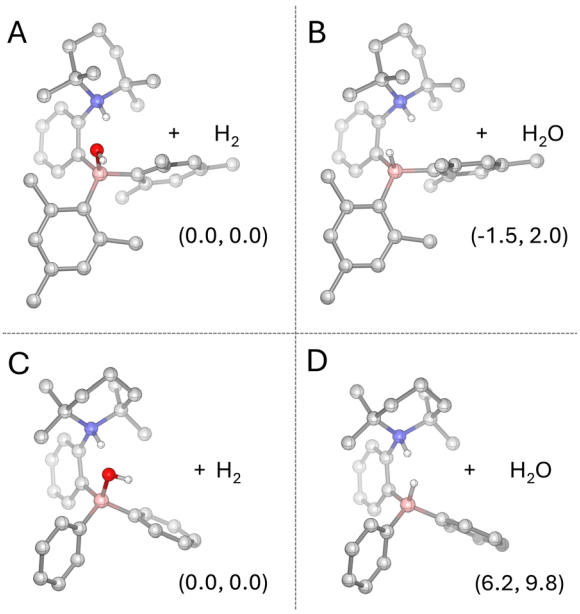

Fig. 3 Comparison of thermodynamic stabilities of **MesCAT** (A) and (B) and **PhCAT** (C) and (D) adducts with water (A) and (C) and dihydrogen (B) and (D) according to the DFT calculations. Structures of the most stable water and dihydrogen adducts are shown in the figure. Relative standard Gibbs free energies, $\Delta_r G^\circ$, in kcal mol^{-1}, are given in parentheses with respect to AAB-H_2O + H_2 for acetonitrile (first number) and toluene (second number) as solvents. To preserve the total number of atoms unchanged, the energies of the AAB-H_2O + H_2 and AAB-H_2O + H_2O states are compared. In the calculation, however, all molecules were treated as separate species (see ESI† for details).

To gain additional insights into the observed differences of the studied AABs, we performed a density functional theory (DFT) modelling of water addition to **MesCAT** and **PhCAT** in acetonitrile and toluene. The geometry optimizations and estimations of solvation effects using the SMD model were performed at the ωB97X-D/6-311G** level of theory similarly as it was done in our previous publications (see ESI† for more details).[11,15] For comparison, Fig. 3 illustrates the most stable structures of AAB-H_2O and AAB-H_2 adducts according to the computations. In the figure, relative standard Gibbs free energies for AAB-H_2O + H_2 (Fig. 3A and C) and AAB-H_2 + H_2O (Fig. 3B and D) are given in parentheses for acetonitrile (first number) and toluene (second number), describing the preference of hydration and dihydrogen addition, respectively. Note that the energies were calculated with respect to the corresponding AAB-H_2O + H_2 level.

Interestingly, the comparison between **MesCAT-H_2O** + H_2 (Fig. 3A) and **MesCAT-H_2** + H_2O (Fig. 3B) reveals quite neutral thermodynamic stability of water and dihydrogen adducts since the $\Delta_r G^\circ$ between the hydrated and the hydrogenated forms of **MesCAT** does not exceed ± 2 kcal mol^{-1}, and both forms can be present in sensible quantities in acetonitrile and toluene. This result supports the experimentally observed thermal and hyperpolarized **MesCAT-H_2** in the water-containing solvents. Specifically, DFT computations imply that under standard conditions in acetonitrile (*i.e.*, 298 K and 1 M concentrations), **MesCAT-H_2** is more favorable than **MesCAT-H_2O** ($\Delta_r G^\circ = -1.5$ kcal mol^{-1}). In contrast, in toluene, **MesCAT-H_2O** is more favorable ($\Delta_r G^\circ = 2$ kcal mol^{-1}). However, the

free energies do not differ significantly, and experimentally, in both cases we have observed hyperpolarization effects. In the case of **PhCAT**, the situation is significantly different, since **PhCAT-H_2O** species are at least 6 kcal mol^{-1} more favorable than **PhCAT-H_2** ($\Delta_r G^\circ$ is 6.2 kcal mol^{-1} in acetonitrile and 9.8 kcal mol^{-1} in toluene). Therefore, in both solvents, the inactive hydrated form of **PhCAT** must be thermodynamically stabilized. This conclusion is clearly confirmed in our experiments, highlighting the relevance of the theoretical approach utilized. We note, however, that DFT predictions have intrinsic precision, which, from our experience with reactivity modeling of AABs, amounts to *ca.* 1 kcal mol^{-1}. Generally, the unique reactivity of **MesCAT** can be attributed to a well-balanced combination of electronic effects – facilitating the sufficient Lewis acidity of the boryl site to activate both H_2 and H_2O – and the steric bulkiness of mesityl substituents. In the case of H_2O, the latter likely induces back strain at the boron site upon hydration, preventing full boron pyramidalization and the formation of a strong B–OH bond, making hydration reversible. The importance of back strain in water tolerance was previously demonstrated by Soós *et al.* for tri(aryl)boranes.[24]

In conclusion, we have demonstrated that nuclear spin hyperpolarization effects with amine-borane frustrated Lewis pairs can be observed in the presence of a dramatic excess of water in solution. To the best of our knowledge, this is also the first communication reporting pronounced water tolerance with this class of metal-free dihydrogen activators. Namely, orthophenylene AAB species with mesityls at the boryl site, **MesCAT**, showed more than three orders of magnitude of ^{1}H NMR signal enhancement in a 9.4 T magnetic field for the **MesCAT-H_2** dihydrogen adduct produced in para-H_2 activation in the presence of a 100-fold excess of water in acetonitrile. Alike results were obtained in the experiments with **MesCAT** in toluene. The performed kinetics measurement provided lifetimes of **MesCAT-H_2** that are significantly longer than those for **MesCAT-H_2O**, confirming the conclusions stemming from the PHIP experiments about the comparative stability of both species. Generally, we can conclude that **MesCAT** can be exposed to air during sample preparation for PHIP experiments or for potential catalytic applications since its water adduct can dissociate in a facile manner, releasing the active free **MesCAT** species. In contrast, **PhCAT** AAB with less bulky phenyl substituents at the boryl site forms very stable **PhCAT-H_2O** adducts due to the irreversible hydration, which disables any PHIP effects with **PhCAT** in the presence of moisture. The performed DFT modelling supported the essential role of steric effects on the way to the optimization of AAB active centers for water-tolerant metal-free dihydrogen activators. Finally, we believe that further rational design of AABs can result in significantly more pronounced shifting of underlying equilibria towards the desired dihydrogen activation and suppressing the formation of the inactive hydration products.

This work was done through the following contributions: K. K.: investigation, validation, writing – review and editing; T. R.: conceptualization, funding acquisition, resources, supervision, validation, writing – review and editing; V. V. Z.: conceptualization, funding acquisition, resources, supervision, investigation, validation, visualization, writing – original draft.

K. K. and V. V. Z. are grateful for the financial support from the Research Council of Finland (grant number 362959) and Kvantum Institute (University of Oulu). V. V. Z. wishes to acknowledge CSC – IT Center for Science, Finland, for computational resources (CSC project 2004016).

Data availability

The data supporting this article have been included as part of the ESI.† In addition, data for this article, including raw NMR data folders and output files for the DFT computations, are available at fairdata.fi at **https://doi.org/10.23729/be2203c4-430c-45f6-aa43-7fb1292dc855**.

Conflicts of interest

There are no conflicts to declare.

Notes and references

1 D. W. Stephan, *Science*, 2016, **354**, aaf7229.
2 A. R. Jupp and D. W. Stephan, *Trends Chem.*, 2019, **1**, 35–48.
3 J. Lam, K. M. Szkop, E. Mosaferi and D. W. Stephan, *Chem. Soc. Rev.*, 2019, **48**, 3592–3612.
4 D. W. Stephan, *Acc. Chem. Res.*, 2015, **48**, 306–316.
5 D. W. Stephan and G. Erker, *Angew. Chem., Int. Ed.*, 2015, **54**, 6400–6441.
6 V. Sumerin, F. Schulz, M. Atsumi, C. Wang, M. Nieger, M. Leskelä, T. Repo, P. Pyykko and B. Rieger, *J. Am. Chem. Soc.*, 2008, **130**, 14117–14119.
7 F. Schulz, V. Sumerin, S. Heikkinen, B. Pedersen, C. Wang, M. Atsumi, M. Leskela, T. Repo, P. Pyykko, W. Petry and B. Rieger, *J. Am. Chem. Soc.*, 2011, **133**, 20245–20257.
8 K. Chernichenko, Á. Madarász, I. Pápai, M. Nieger, M. Leskelä and T. Repo, *Nat. Chem.*, 2013, **5**, 718–723.
9 V. Sumerin, K. Chernichenko, M. Nieger, M. Leskela, B. Rieger and T. Repo, *Adv. Synth. Catal.*, 2011, **353**, 2093–2110.
10 K. Chernichenko, M. Lindqvist, B. Kótai, M. Nieger, K. Sorochkina, I. Pápai and T. Repo, *J. Am. Chem. Soc.*, 2016, **138**, 4860–4868.
11 K. Chernichenko, B. Kótai, I. Pápai, V. Zhivonitko, M. Nieger, M. Leskelä and T. Repo, *Angew. Chem., Int. Ed.*, 2015, **54**, 1749–1753.
12 V. V. Zhivonitko, K. Sorochkina, K. Chernichenko, B. Kotai, T. Földes, I. Pápai, V.-V. Telkki, T. Repo and I. Koptyug, *Phys. Chem. Chem. Phys.*, 2016, **18**, 27784–27795.
13 K. Sorochkina, V. V. Zhivonitko, K. Chernichenko, V. V. Telkki, T. Repo and I. V. Koptyug, *J. Phys. Chem. Lett.*, 2018, **9**, 903–907.
14 D. O. Zakharov, K. Chernichenko, K. Sorochkina, S. Yang, V. V. Telkki, T. Repo and V. V. Zhivonitko, *Chem. – Eur. J.*, 2022, **28**, e202103501.
15 K. Konsewicz, G. Laczkó, I. Pápai and V. V. Zhivonitko, *Phys. Chem. Chem. Phys.*, 2024, **26**, 3197–3207.
16 C. R. Bowers and D. P. Weitekamp, *Phys. Rev. Lett.*, 1986, **57**, 2645–2648.
17 C. R. Bowers and D. P. Weitekamp, *J. Am. Chem. Soc.*, 1987, **109**, 5541–5542.
18 C. R. Bowers, in *Encyclopedia of Nuclear Magnetic Resonance*, ed. D. M. Grant and R. K. Harris, Wiley, Chichester, 2002, vol. 9, pp. 750–769.
19 B. J. Tickner and V. V. Zhivonitko, *Chem. Sci.*, 2022, **13**, 4670–4696.
20 S. B. Duckett, in *Encyclopedia of Spectroscopy and Spectrometry*, ed. J. C. Lindon, G. E. Tranter and D. W. Koppenaal, Elsevier, 2016, pp. 527–534.
21 K. Sorochkina, K. Chernichenko, V. V. Zhivonitko, M. Nieger and T. Repo, *Chem. – Eur. J.*, 2022, **28**, e202201927.
22 K. Sorochkina, K. Chernichenko, M. Nieger, M. Leskelä and T. Repo, *Z. Naturforsch., B*, 2017, **72**, 903–908.
23 V. Fasano and M. J. Ingleson, *Synthesis*, 2018, 1783–1795.
24 É. Dorkó, M. Szabó, B. Kótai, I. Pápai, A. Domján and T. Soós, *Angew. Chem., Int. Ed.*, 2017, **56**, 9512–9516.
25 Á. Gyömöre, M. Bakos, T. Földes, I. Pápai, A. Domján and T. Soós, *ACS Catal.*, 2015, **5**, 5366–5372.

